buildings

MDPI

Article

Design of an Instant Vibration-Based Warning System and Its Operation during Relocation Works of Historic Facades

Antolin Lorenzana *, Juan Jose Villacorta, Alvaro Magdaleno, Lara del Val and Alberto Izquierdo

ITAP (Instituto de las Tecnologías Avanzadas de la Producción), Universidad de Valladolid, 47002 Valladolid, Spain; juanjose.villacorta@uva.es (J.J.V.); alvaro.magdaleno@uva.es (A.M.); lara.val@uva.es (L.d.V.); alberto.izquierdo@uva.es (A.I.)

* Correspondence: antolin.lorenzana@uva.es

Abstract: Preserved listed building facades may require large-scale and highly technical work when the supporting building structure is at serious risk of collapse. Such is the case described in this paper, where vast facades must be cut into large panels up to 200 m^2 and 150 t in weight and carefully laid on the ground. Various engineering works must be carried out to ensure the structural integrity of the panels to be safeguarded. Each panel must be reinforced by a temporary lattice steel structure prior to the disengagement from the supporting building frame. The operations require the use of cutting tools, hitting demolition machines and heavy cranes, which can induce potentially damaging vibrations that should be monitored and processed so that workers can be alerted in real time if certain thresholds are exceeded so that they can proceed more carefully. The paper describes the specifically designed monitoring system, its electronic parts, how they operate and how the data are processed and displayed. The monitoring system, once verified in laboratory tests, is applied to the detachment and overturning activities of a representative full-scale panel, tracking vibration levels and tilting rates. After days of operation and visual observation, it is possible to correlate vibration levels with incipient damage, establishing that peaks below 0.5 m/s^2 or RMS values of 0.05 m/s^2 are permissible, but that above 1.0 m/s^2 or 0.3 m/s^2, respectively, activities should be halted. The proposed system has proven to be useful for the intended purposes, making it possible to know the acceptable thresholds and trigger the necessary alarms in real time for the successful course of the work.

Keywords: heritage facade preservation; deconstruction work; structural health monitoring; mosaic damage; shock and vibration

Citation: Lorenzana, A.; Villacorta, J.J.; Magdaleno, A.; Val, L.d.; Izquierdo, A. Design of an Instant Vibration-Based Warning System and Its Operation during Relocation Works of Historic Facades. *Buildings* **2024**, *14*, 1889. https://doi.org/10.3390/buildings14071889

Academic Editors: Rui Marques, Claudia Mondelli and Maria Giovanna Masciotta

Received: 24 May 2024
Revised: 17 June 2024
Accepted: 18 June 2024
Published: 21 June 2024

1. Introduction

Certain heritage conservation work may entail risks that need to be monitored. From a structural point of view, these risks are associated with structural vibrations whose frequency and amplitude content must be tracked. The long-term monitoring systems based on accelerometer sensors provide the best method to track and quantify the real environmental loads and the corresponding structure response affecting their integrity [1,2]. Multiple examples of structures equipped with different types of monitoring systems are well documented in thousands of papers, including peer-reviewed specific scientific journals covering this field of engineering (e.g., structural health monitoring, established in 2002), where the evolution in performance and cost of the different proposals is evident. A number of short-term monitoring situations are also documented [3,4], such as that which is the subject of this paper. The main problems for making the implementation of these monitoring systems more widespread are not only the cost associated with the purchase and installation of the measuring system (sensors, acquisition equipment, wires, etc.) including its operation maintenance but also the need for both the hardware and software to be adapted to each particular construction site. Various papers, including reviews [1,5,6],

try to highlight the advantages and disadvantages of some systems over others, matching piezoelectric sensors versus MEMS (which stands for microelectromechanical systems), since they first appeared in the 1990s, or wired versus wireless systems (with the advent of the Internet of Things (IoT) paradigm from 2005 onwards). However, all these technologies can be accommodated depending on the application, or they can even coexist, as in the case proposed here. There are also numerous examples [2,7,8] where structural health monitoring (SHM) needs are also covered by low-cost systems and combined with multi-platform information and warning systems [9–11].

Regarding the protection of cultural assets from mechanical loads, Refs. [12,13] apply different criteria to establish the admissible thresholds for the different assets (painting canvasses, figures, wall paintings, etc.) for their conservation under normal exhibition, transportation or storage conditions. Other researchers (such as [14]) specifically analyse the effect of construction work (site clearing, excavation, drilling of micropiles, etc.) near museums and depots. In all these works, metrics defined in various vibration standards (such as BS 5228-1 [15], BS 7385-2 [16] and DIN 4150-3 [17]) or human exposure to vibration standards (such as BS 6472-1 [18] or ISO 2631-1 [19]) are proposed, which are not directly applicable to the facade movement activities under study. Some works on how to protect museum collections against vibrations due to construction works (such as [20,21]) are also interesting, but the different solutions are also not practical given the size of the facades.

Although many SHM systems are designed for permanent installation during the lifetime of the structure, there are numerous recent examples where they are installed during conservation work [22,23] or even with the intention of monitoring during deconstruction or demolition. Most examples are for bridges or large infrastructures [3,4,9,10,24–27], although they are also starting to be used in civil buildings with the aim of reuse [11], even combined with modern BIM-based applications for waste management and recycling [28–30].

With all this background and their experience in vibration monitoring [2,31], the authors are proposing the design of a novel system capable of tracking the tilting rates and the vibration level at up to six points and warning at the construction site if some metric exceeds the predetermined thresholds. The sensors, MEMS type [31,32], are wired to the cabinet where they are processed (to evaluate metrics and to manage the alarms) and temporarily stored and can simultaneously be uploaded to platforms (thanks to the Wi-Fi connectivity installed on site) for final storage and post-processing, if necessary. The main advantage of the alternative system is, apart from its low cost, its flexibility, as it is developed ad hoc (hardware and software) under the specific requirements for the on-site operation.

After this introduction, the paper continues with a description of the designed system (Section 3) for its application to the construction site, whose main activities are also briefly described in Section 2 for better contextualisation. It continues with the methodological proposal on the basis of which some thresholds are established and the alarm system is managed (Section 4). The last Sections (Sections 5 and 6) present the laboratory verification and different real events on site, which give an idea of the capabilities of the equipment developed and the vibration levels that can be expected in this type of deconstruction operation. The paper concludes by summarising the methodology and highlighting the main conclusions (Section 7).

2. Deconstruction Plan and Work on Site

The heritage element to be safeguarded (large Mexican mosaics) is integrated along several facades covering a large area of a federal building belonging to Mexico's Ministry of Infrastructure, Communications and Transport (SICT). The facade is a structural part of the reinforced concrete building to which it belongs, built in the 1950s. Obviously, at that time, the structures were not built with their easy dismantling in mind, the basis for which has been laid in recent decades [33]. Once the authorities decided to demolish the building, aged and severely damaged by several earthquakes, a plan was established to recover the mosaics integrated into the facades. This plan consisted of partitioning the facade into

multiple panels of the largest possible dimensions in order to minimise damage during the sectioning process (wire cutting). Although the work is very varied, a panel with the dimensions of 20 m high and 10 m wide is considered as a reference in this description. With these large dimensions, each panel does not have on its own enough stiffness and, to ensure its structural integrity, it is reinforced by adding a temporary lattice steel structure (abbreviated as TLSS). The weight of the assembly must not exceed the capacity of the cranes (up to 700 t) with which it will be lifted and subsequently overturned, this being another one of the criteria that determine the size of each panel.

To contextualise the work, accurately describe the process, understand the warning developed system and interpret the figures presented in this paper, each facade is considered to be vertical and contained in the plane XY, with X being the vertical axis and Y the horizontal one, as shown in Figure 1a. The typical detachment process of a facade panel is conceptually described as follows: Note that the facade houses a large mosaic, composed of small tesserae. Panels up to 10 × 20 m^2 are identified and are to be separated from the rest of the facade by means of straight cuts made with wire saws. With such dimensions, the panels are clamped to the structural frame of the building mainly through the edge of the floor slabs. As the panels are fragile, before separating them from their supports and once protected with various surface coatings, they are reinforced by the TLLS on both sides, connected to each other through holes bored in the facade itself. Before cutting or trepanning, the tesserae that could be affected by those events' operations are identified and removed for subsequent replacement. The panel, forming a rigid sandwich with its protective TLSS, is still connected to the rest of the building through the heads of the floor slabs. Work is required to release the sandwich assembly from the building frame. During these works, for safety reasons, the sandwich is held in place by the slings of the corresponding auto crane. The works consist of cutting (using wire saws), trepanning and demolition (using drilling machines and jackhammers) and the use of flame-cutting systems for the steel parts. All these activities induce potentially damaging vibrations. Once the panel has been released, it is hung from the auto crane, which then moves it away from the building (with rotation movements) and then tilts. Figure 1b shows a turn with respect to the X axis followed by a 90° turn with respect to the Y axis (Figure 1c), after which the panel lies flat on the ground. This last job is carried out with the help of a second crane to ensure the smoothest possible movements. In spite of this, vibrations may occur during all the processes due to, among other eventualities, the necessary manoeuvring of the cranes, possible impacts with the building or the ground supports or the readjustment of the slings on their lugs during the tilting manoeuvre.

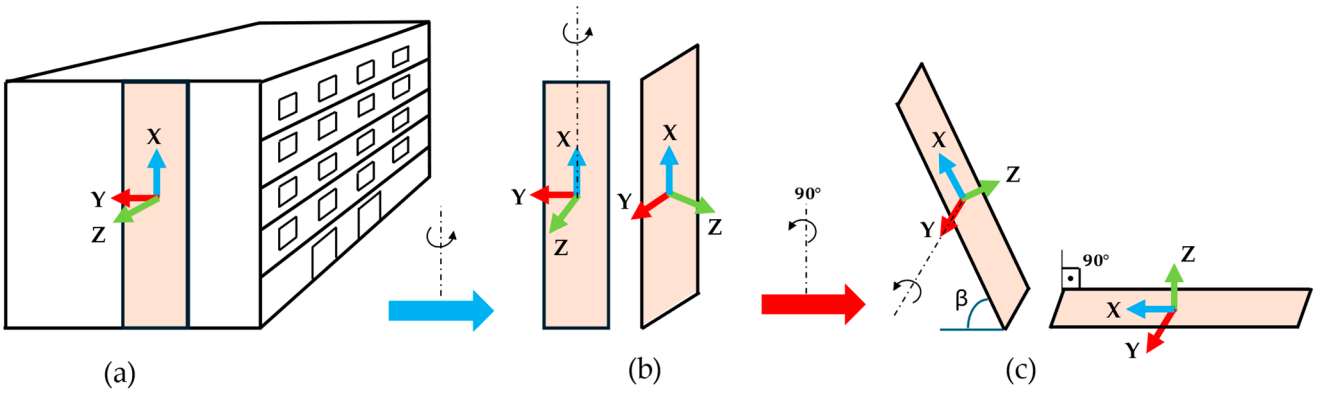

Figure 1. Conceptual sequence of the process of detachment of a facade panel. (**a**) Identification of a panel within a facade; (**b**) illustration of some handlings with respect to the X axis; and (**c**) depiction of the tilt process (rotation about the Y axis).

3. Monitoring System: Cabinet and Sensor Description

The heart of the instrumentation system is shown in Figure 2. The equipment must be compact, watertight, rugged (IEC 60529 IP65 [34]) and manageable by a single worker so

that it can withstand on-site rough play and weather conditions and be relocated panel after panel. All these features are achieved with the shown electric cabinet, which contains the datalogger (1) and incorporates the acoustic and visual warning system (2), together with other necessary electrical devices, such as connectors and relays (3). Outside the cabinet, connected by wires, are six boxes (also IP65) housing, each one, the vibration sensor (4). The whole unit is powered (5) either by a powerline or with the corresponding power bank. Note that the use of the system should not add additional risks during the practical execution of the work, carried out in accordance with the Mexican Occupational Safety and Health Conditions (NOM-031-STPS-2011).

Figure 2. Cabinet including datalogger (1), beacon (2), connectors and relays (3), vibration sensors (4) and power supply (5).

The vibration sensor is based on the ADXL355 digital MEMS developed by Analog Devices (Wilmington, MA, USA). This sensor is a very small, low-noise, low-drift and low-power 3-axis accelerometer that can measure the static acceleration of gravity as well as dynamic acceleration at a high sampling rate. The accelerometer properties (shown in Table 1) are initially suitable to measure the expected dynamic response (in frequencies and amplitudes). Properly conditioned and integrated with an analogue-to-digital converter (ADC), digital data are sent over a 10 m cable Ethernet Cat. 5e. The sampling rate for each channel is adjustable, set by default to 125 Hz, adequate to the intended purposes, including the possible estimation of the modal parameters of the structure, where the first bending modes are below 25 Hz, thus avoiding aliasing problems.

Table 1. Main characteristics of the accelerometers.

Characteristic	Value
Accel. range	±2 g
Accel. digital sensitivity	3.9 μg/LSB
Accel. noise density	25 $\mu g/\sqrt{Hz}$
Max. sample frequency	4 kHz
Bits per sample	20
Bandwidth	0 Hz–1500 Hz

Up to six of these sensors are wired to the acquisition system, which is based on a myRIO® (National Instruments, Austin, TX, USA) device from National Instruments. This device uses a Xilinx Zynq 7010 chip (Xilinx, San Jose, CA, USA) that is composed of a Field-Programmable Gate Array, or FPGA, used to register data from the accelerometers, and a dual-core ARM® Cortex™-A9 processor (Arm, Cambridge, UK) that processes the acquired data in order to extract several metrics, such as acceleration amplitudes, prevalent

frequencies and the rate of change in the tilt angles. If the adjusted thresholds are exceeded, the system generates different codified alarm outputs ranging from light signals of different colours and cadences to sounds with different tones and intensities. The device includes local storage where both raw acceleration data and their metrics are saved. Although data are continuously stored, each one of the final files contains 15 min of registered data. This size has been selected as a trade-off between the management complexity associated with dealing with multiple files and the overload that may occur if too large files are to be handled by the monitoring system. Since it is a system designed to operate continuously, the stored data consume the available capacity, so when the maximum is reached, the new data replace the old data. However, greater persistency of the relevant data (associated with an alarm) is achieved by sending it to a dedicated remote server. To perform this work, the device incorporates Wi-Fi connectivity, which makes it ideal for the proposed application.

To visualise the monitoring results on different mobile devices, the metrics (and the alarms) are also sent to a remote database, for which it is essential that the Wi-Fi interface is connected to the internet via a proper access point. This aspect implied serious drawbacks, as the construction site to be monitored extends over a large area with many buildings between the access point and the monitoring systems, exceeding the standard range of a conventional Wi-Fi node. The final solution was to deploy a set of mesh-type Wi-Fi transceivers to guarantee full coverage.

Being connected to the internet, logs and alarms can be viewed on different platforms, but the on-site functionality also requires a quick warning to the construction workers. The warning system consists of a beacon (from Auer Signal® (Wien, Austria)), capable of lighting up in up to seven different colours to indicate different system statuses, also including a buzzer playing audible warnings. The management of these two elements is regulated by a set of solid-state relays controlled by the myRIO® device.

The tracking of accelerations is done in each local axis, dependent on the positioning of the box on the surface of the panel. To facilitate data interpretation, efforts must be made to place each box according to the vertical XY plane (Figure 1) and thus avoid matrix operations to shift to the global axes. This makes it much easier to process the data from which the tilt angles were extracted.

4. Methodology and Threshold Setting

The processing system implements an actor-based architecture that allows the parallel execution of different processing elements, providing communication and synchronisation mechanisms between them while keeping down the use of resources. The main actors defined in the system are the following:

Acquisition: this is responsible for setting up the sensors connected to the system and synchronously reading the multi-axis acceleration data at the defined sampling rate (125 S/s by default) and saving it to the local storage memory. The signal conditioning, processed within each digital MEMS sensor (4), includes analogue anti-aliasing low-pass filtering, analogue-to-digital conversion and digital decimation with a digital low-pass filter.

Processing: when a dataset of a preset length (variable for each metric) has been acquired, this actor evaluates the following values: regarding the relative vibrations, after eliminating the continuous component by means of a high-pass filter, for each axis of each sensor, the maximum or peak acceleration (of the last 1 s period, this period being settable), its root mean square value (RMS, of the last 30 s period) and the most significant frequencies (by means of the fast Fourier transform (FFT) of the last 30 s period) are evaluated; regarding the tilt, with the raw (unfiltered) X or Z axis records of one of the accelerometers (for this purpose they all offer similar values), the angle with respect to the vertical (β in Figure 1) is evaluated and its rate of change is averaged. All these metrics are indexed for their tracking over time.

Warning management: this actor compares the processed metrics with the corresponding previously established thresholds and generates an alarm when any threshold is exceeded. Three types of alarm are distinguished, depending on the metric that is exceeded:

maximum amplitude, RMS values and tilt ratio. For the application under consideration, where the eigenfrequencies are changing markedly as the panel is being released, no thresholds have been necessary to track prevailing frequencies. Thresholds are configurable both per sensor and per axis, with different alarms generated for each element. The beacon remains green if no alarm has occurred; otherwise, it alternates between different encodings (colours and cadence of flashes). Figure 3 summarises one of the proposed configurations, among many other possibilities. This proposal corresponds to slow red flashing from 0.1 to 0.5 m/s^2 for the peak metric, faster red flashing from 0.5 to 1 m/s^2 and steady red light for greater values. Once an alarm is triggered, it remains active for the following 10 s, unless it needs to upgrade to a higher intensity one. In addition to the light signals, a buzzer can be operated if necessary.

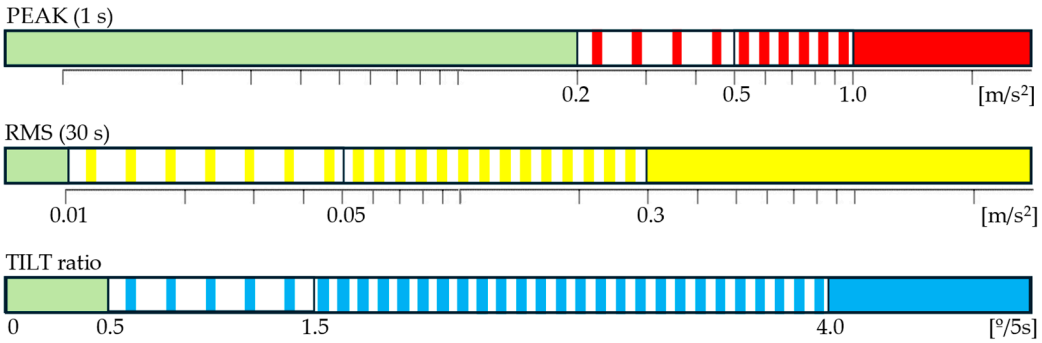

Figure 3. Thresholds and coding of the beacon for peak acceleration values (in red), RMS (in yellow) and tilt ratio (in blue).

Storage: all computed metrics, as well as the generated alarm codes, are stored in a remote database ready to be displayed on mobile platforms. To minimise communications, all results from a configurable time interval (set to 10 min by default) are grouped in a single block to be uploaded, but each event with its corresponding timestamps.

Raw data transfer: when any alarm occurs, the raw acceleration data of the sensor and axis that caused the alarm are sent to the remote database for in-depth offline analysis. The length of that record, prior to the alarm event, is configurable, set to 15 min by default.

The system includes other actors in charge of verifying the performance of the sensors and the operative conditions of other components. It also provides a user interface for management (setting times and thresholds) and updating the firmware, if necessary.

5. Lab Testing

In order to tune up the new system, several tests have been carried out in a laboratory environment. In [31], the system's features for modal analysis were validated by comparison with piezoelectric accelerometers and commercial dataloggers. For the application of this work, it was also necessary to verify its suitability to measure inclination (and their rate of change) to ensure their slow evolution during the tilt process. The idea was based on the concept that the MEMS registers the acceleration of gravity and, therefore, the same sensor can be used either to process the vibrations (once the continuous component has been filtered out) or to evaluate the tilt.

For this verification, the following case study was proposed (see Figure 4): the system (left, vibration sensor 1 and datalogger 3) is mounted on a small wooden board ($2.5 \times 1.25 \times 0.02$ m^3), to which an inclinometer (2), based on Movella® DOT technology, is coupled; starting with the board in a vertical position, it is then turned over by rotating the assembly with respect to the local Y axis (Figure 1c) in a sequence lasting approximately 24 s, as can be seen in Figure 5. In addition, to ensure its functionality under operating conditions in the construction site environment with noise and vibrations, the board was exposed to certain vibrations induced by light knocks during the tilting process. The acceleration records start with values of g (about 9.8 m/s^2) on the X-axis (a_X) and close to zero on the Z-axis (a_Z).

As the tilt progresses, the inclination at each instant can be calculated either by looking at how the X component decreases down to zero or how the Z component increases (from zero to the value of g). In the first case, the Equation (2) is used, and in the second case, the equation to use is Equation (3). Note that, in the above, the acceleration modulus must be calculated in the usual way, as stated in Equation (1), regardless of the vibrations that may occur.

$$|a| = \sqrt{a_X^2 + a_Y^2 + a_Z^2} \tag{1}$$

$$\sin \beta_X = \frac{a_X}{|a|} \tag{2}$$

$$\cos \beta_Z = \frac{a_Z}{|a|} \tag{3}$$

Figure 4. Tilting testing: dual instrumentation and lab set-up. (1) Vibration sensor, (2) inclinometer and (3) myRIO device.

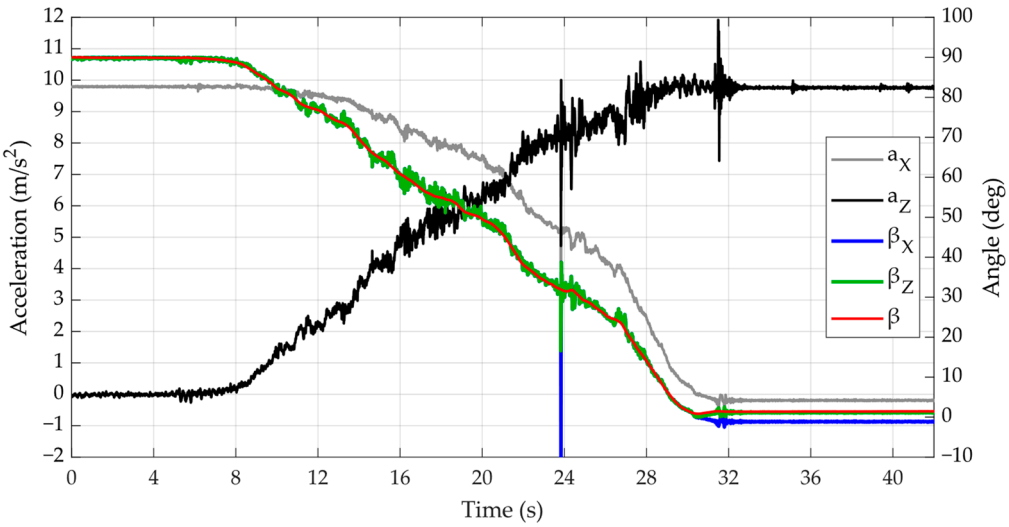

Figure 5. Tilting test: accelerations and angles.

Proceeding in this way, both Equation (2) and (3) are equivalent (in fact, in Figure 5, they overlap). Moreover, they coincide with the inclination provided by the inclinometer (β angle in Figure 1c), which in fact offers average values obtained by means of strapdown integration procedures of the set of the recorded kinematic magnitudes [35,36]. For the purpose of validating the procedure, no filters or smoothing algorithms have been applied in Figure 5. This makes pertinent the statistical analysis presented in Figure 6, which also shows, for each measured data, the differences between both values (β_Z and β, from the inclinometer) as the tilt progresses. It is assumed that the average deviation of 0.133° (black line) is due to the lack of perfect initial alignment between the MEMS sensor and the inclinometer (which is also a MEMS sensor). What is more interesting is to see that the $\pm 1.96\sigma$ confidence interval (95% limit of agreement, or LoA) assumes an amplitude of only

1.46°, which is more than enough for the purposes of this work. Therefore, it is shown that with the only use of the MEMS accelerometers, both objectives (vibrational status and tilt ratio evaluation) can be achieved.

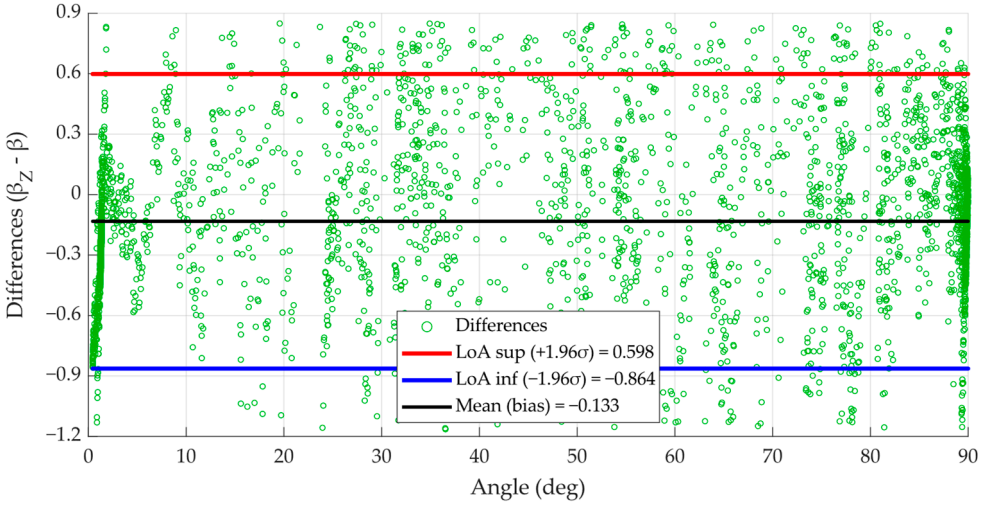

Figure 6. Concordance plot between β_Z and the one provided by the inclinometer sensor.

6. Full-Scale Application

The description made in Section 2 about on-site works and the conceptual sequence in Figure 1 is complemented by eight photographs of one of the scenarios, courtesy of CAV Diseño e Ingeniería, shown in Figure 7. Some of these pictures show the cabinet, the boxes with the sensors and the luminous and acoustic beacon (light green dot in the second photograph of the first row), discussed above. This section will comment on the results of some significant events.

Note that each panel must be monitored for several hours, depending on the works necessary for its detachment and overturning. As a reference, about 10 h for preliminary works (installation of the protective coatings and the TLSS), another 10 h for the preliminary release works, about 1 h for its complete detachment and about 30 min for its overturning.

Once the monitoring system has been installed in the corresponding panel and is ready to use, it is time to analyse the vibration levels and the tilting process. With the aim of illustrating the levels of vibration under different situations on site, six significant records with increasing levels of acceleration are briefly presented. In all cases, the Z component (perpendicular to the panel, which is the prevailing one) of the acceleration is shown, although X and Y are not negligible, as illustrated in Figure 12 below.

During night hours, without workers on site, Figure 8 shows the minimum level of acceleration, which can be considered ambient noise. Peak values are about 0.004 m/s^2 with RMS values below 0.001 m/s^2.

The response of the same panel during working hours, but without nearby machining activities, is shown in Figure 9. Peak accelerations can reach 0.05 m/s^2 with RMS values around 0.006 m/s^2. These acceleration levels are similar to the case where the panel is being handled in the air, hanging from the crane, as shown in Figure 10. By applying the FFT algorithm, frequencies with structural implications can be obtained and are briefly discussed below. Thus, for example, in Figure 9, there is a predominant peak at 7.58 Hz (Figure 11, in green), which corresponds to a bending mode shape (Z axis) of the TLSS. Other peaks at lower frequencies may reflect the horizontal movements of the building as a whole. In the same way, the FFT analysis of Figure 10 reveals that the significant bending frequency drops to 2.45 Hz (Figure 11, in blue), as the panel supports have changed down significantly.

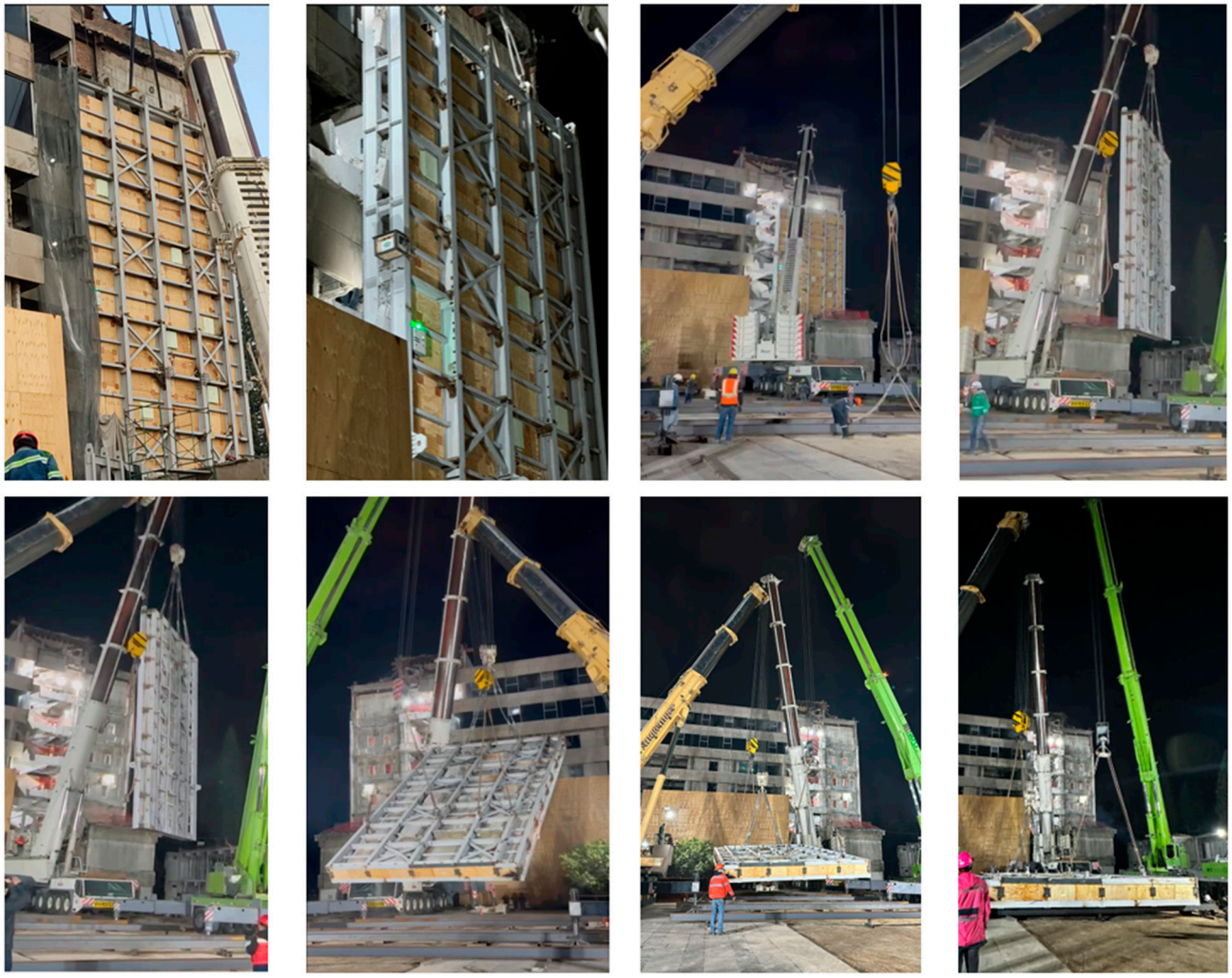

Figure 7. Sequence of photographs corresponding to a specific facade panel.

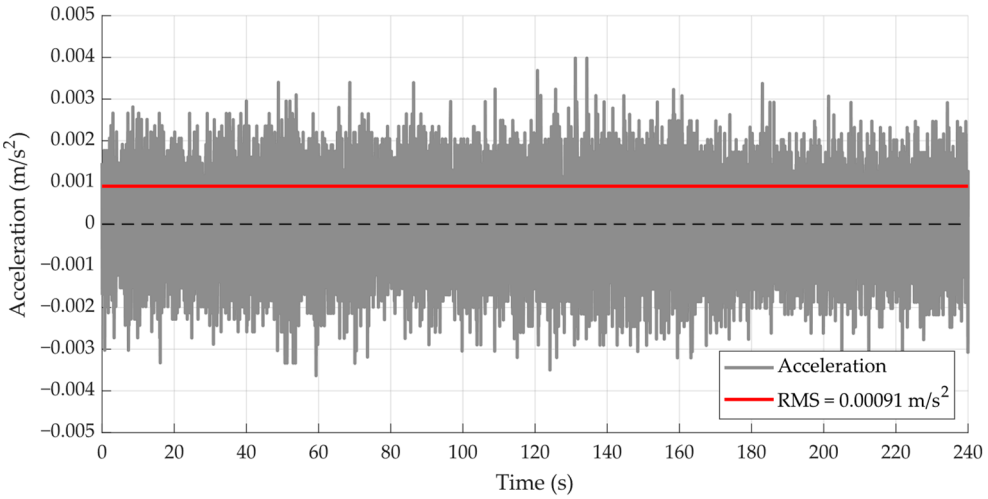

Figure 8. Representative record of the panel with no activity on site (ambient noise).

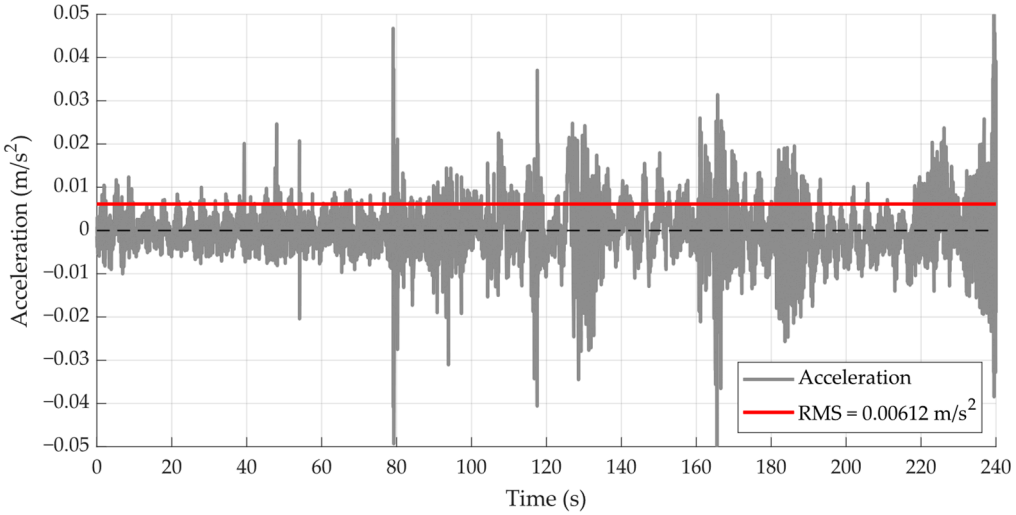

Figure 9. Representative vibrations during distant machining activities on site.

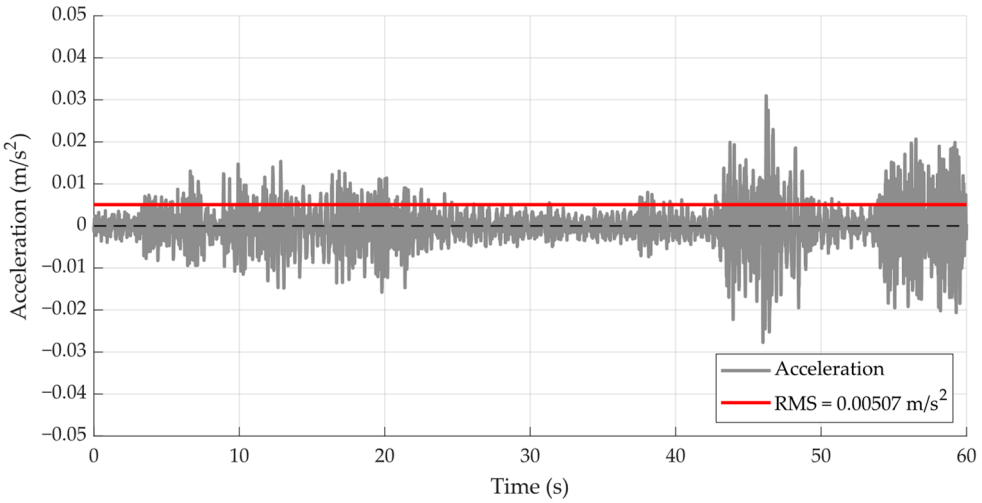

Figure 10. Representative vibrations on a panel hanging from the crane.

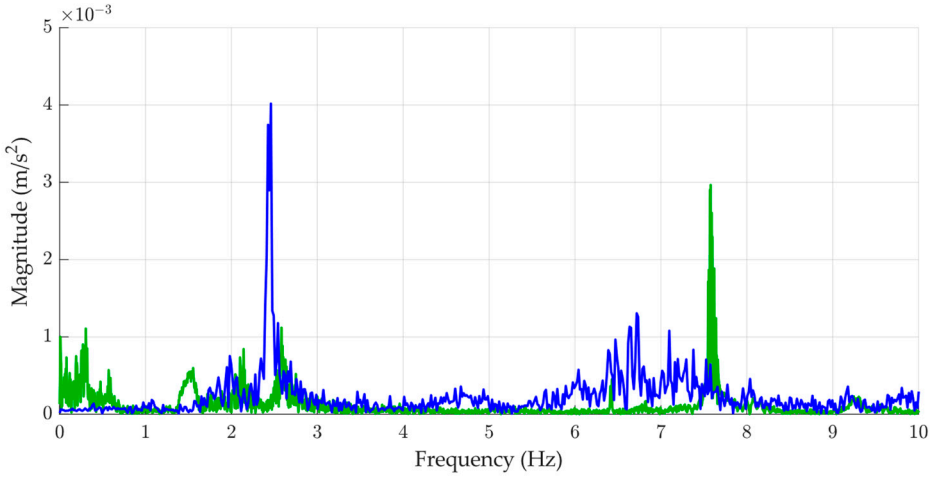

Figure 11. FFT applied to the acceleration records in Figure 9 (in green) and Figure 10 (in blue).

The nearby machining (drilling, cutting and demolition work) required to detach the panel from the building frame causes significantly higher accelerations. Figure 12 shows the recorded accelerations on the panel when jackhammers are acting on the slabs to which

the panel itself is still clamped. Also, the in-plane accelerations (X and Y axis) are added for completeness. The impacts of the hammers occur at intervals of approximately 1 s, causing significant peaks in the panel of values of 0.25 m/s^2, which are quickly damped. The wire-cutting activities do not cause periodic patterns as in Figure 12, but they do cause a noisy record similar to that in Figure 9, but with higher amplitudes, with RMS values of about 0.027 m/s^2 and peaks in the order of 0.12 m/s^2.

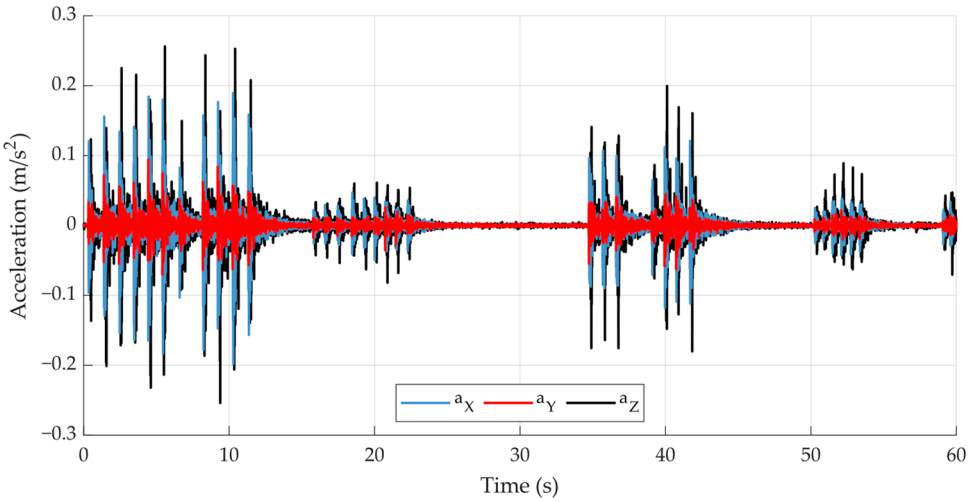

Figure 12. Accelerations when jackhammer is acting just on the slabs that still clamp the panel.

Although the crane, during the detachment work, is progressively loaded with the weight of the panel, just at the instant when the last joint breaks, it is inevitable that the accelerations reach significant levels. Such is the case shown in Figure 13, with an initial peak of 0.5 m/s^2 quickly damped and followed by a typical pendulum as the panel hangs from the auto crane.

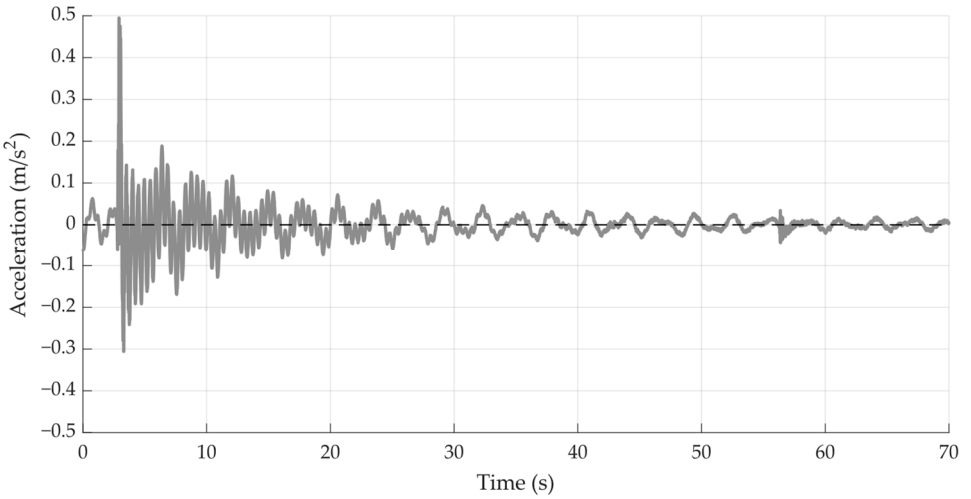

Figure 13. Vibrations at the instant of breaking the last joint between the panel and the building frame.

As an example of a shock event, Figure 14 shows the record corresponding to the instant in which the panel, at the end of the overturning process but still hanging from the cranes, first impacts with the ground support, reaching high peak accelerations of 5 m/s^2, also very quickly damped.

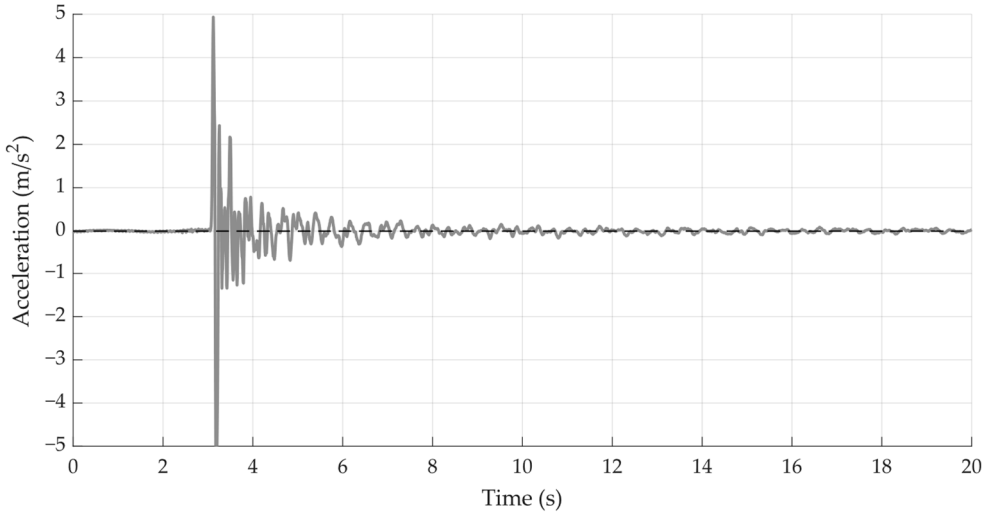

Figure 14. Impact when laying the panel on the ground.

The previous figures are supplemented with Figure 15, where, with no relevant activity at the construction site, an earthquake was clearly recorded on 12 December 2023 at 17:07:52 UTC, magnitude 3.0 on the Richter scale, with the epicentre at coordinates 19.363, −99.200, latitude and longitude in decimal degrees, at a depth of 1 km, only 6.4 km away from the construction site itself, with coordinates 19.394, −99.148. The above event corresponds to the central part in Figure 15, although the Mexican Servicio Sismológico Nacional (SSN) also recorded an 85 s earlier earthquake (17:06:27 UTC) of intensity 2.8 and another 61 s later (17:08:53) of intensity 2.4, which can also be discerned in Figure 15.

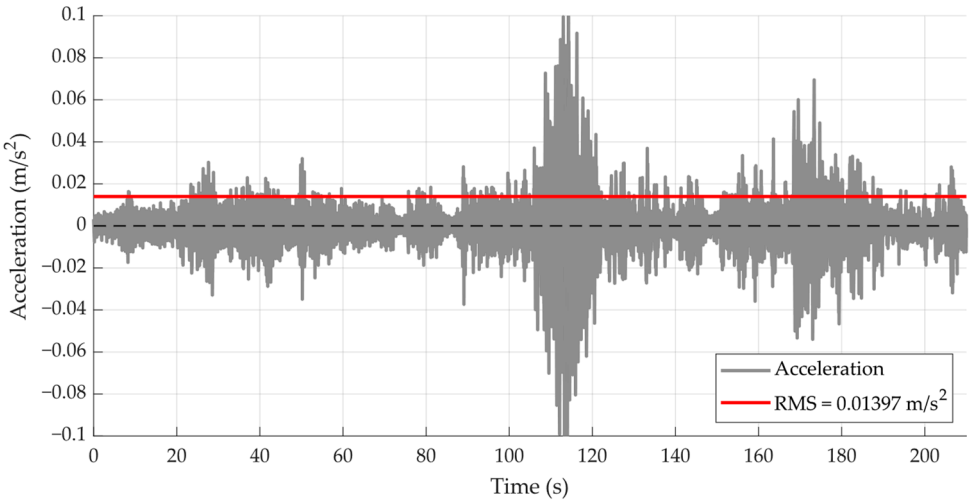

Figure 15. Acceleration on the panel due to nearby (6.4 km) seismological activity.

The complete record (about 30 min) of the overturning of one of the panels is presented in Figure 16, which can be taken as a meaningful reference. The figure includes, in its last seconds, the impact shown in the previous Figure 14. The additional Figure 17 shows, on the same time axis, a detail of the 60 s interval, to appreciate the level of vibrations due to the manoeuvres of the cranes, despite this being done with the maximum smoothness. The highest vibrations are associated with the auto crane vibrations and with the reconditioning of the sling straps inside the lifting lugs, as the angle changes during the process.

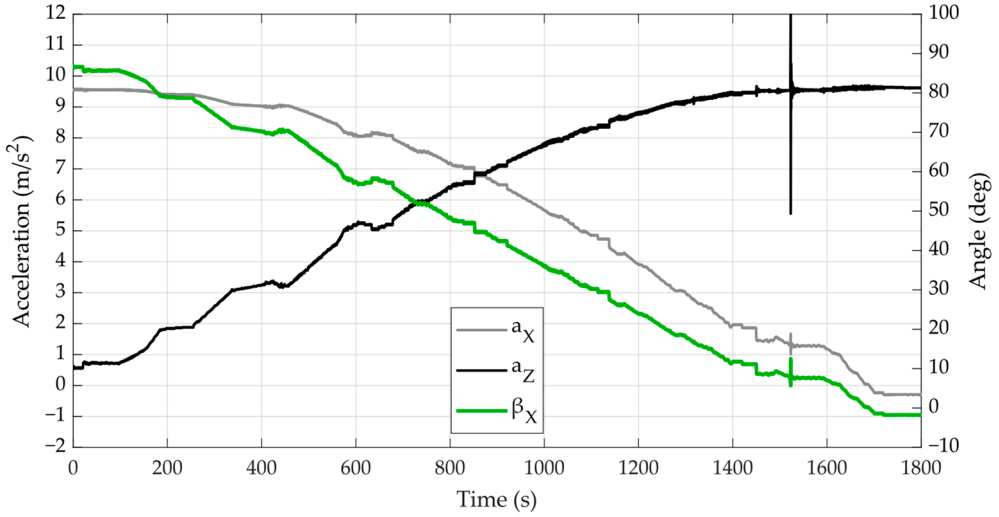

Figure 16. Reference tilting process for an actual panel.

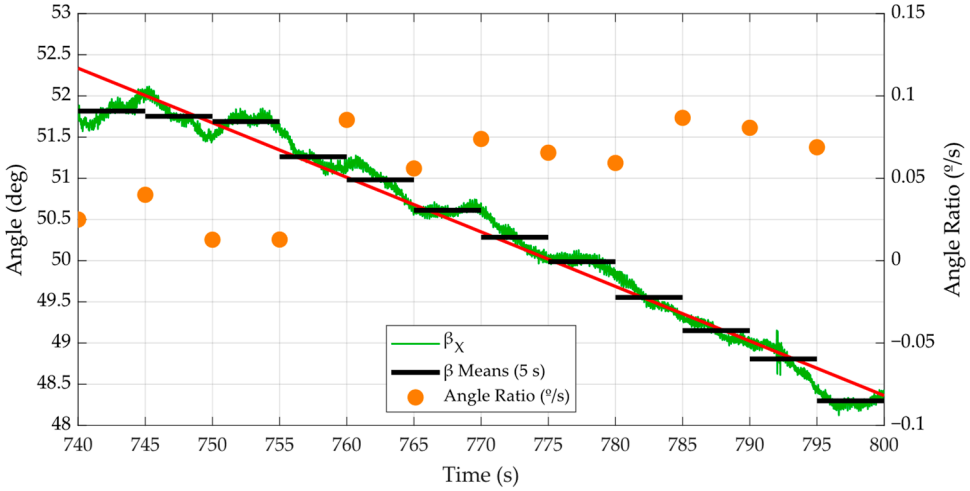

Figure 17. Instant angles (green), averaged values (5 s) (black lines) and ratio (orange dots).

In order to evaluate a reference tilt ratio on the basis of which to make comparisons and to set tilt thresholds, the value of the angle (in degrees) is also shown in detail for a one-minute interval in Figure 17, together with mean values, evaluated every 5 s with the data from the previous 5 s interval. With these values, the rate of change in the tilt angle is also shown in Figure 17, secondary right axis, where the maximum averaged speed is only about 0.12°/s. The figure also shows the regression line (in red) for the actual manoeuvre under study with an average speed (in those 60 s detailed in Figure 17) of only 0.0651°/s. At that speed, it would take about 24 min for the panel to lie on the ground (see also Figure 16). Note that the visible steps in the green line of Figure 17 are due to the necessary stops by the crane operator, as such a slow speed is not compatible with the continuous mechanical drive systems of the crane.

An example of the metrics tracking under analysis during 2 h of work on-site, including most of the activities mentioned above, is presented in Figure 18. At 3200 s, the panel is just hanging on the crane, and the tilting manoeuvre starts. Both peak and RMS values are shown for the Z-axis in the logarithmic scale. The thresholds are also indicated with horizontal lines (the same as those proposed in Figure 3). As some metrics exceed the thresholds, the alarm is triggered for both peak and RMS values. In the event that two alarms are exceeded in the same time interval (at least 5 s), only the one with the maximum relative value is displayed.

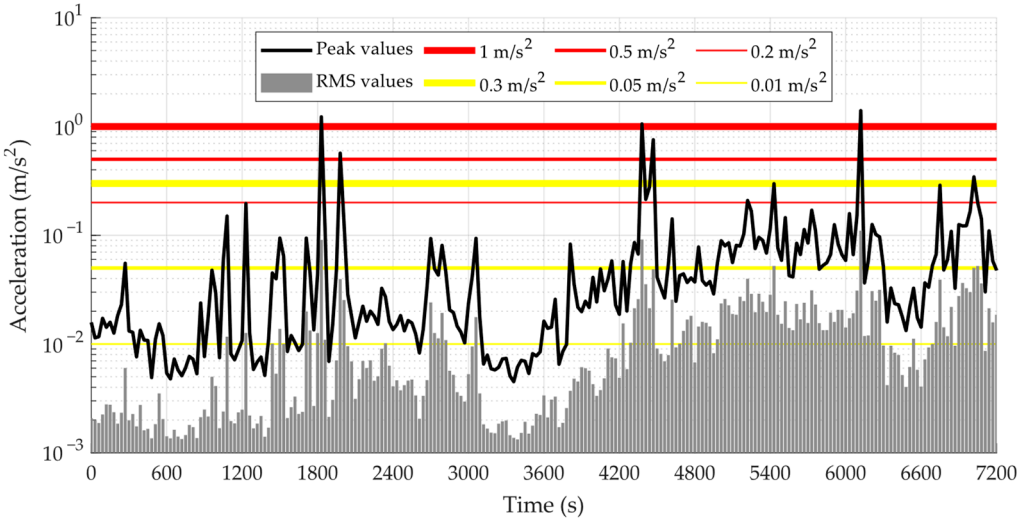

Figure 18. Peak and RMS values tracking during detaching from the building frame and tilting process.

7. Conclusions

The development and operation of a portable vibration monitoring system have been presented in this paper. It is intended to be used during the deconstruction works of the heritage-listed facades of a building severely damaged by previous earthquakes, prior to its demolition. The singularity of the application leads to the need to design a specific hardware and software system that, properly conditioned and embedded inside a portable cabinet, is ready to be used by the site personnel, giving immediate feedback on the progress of the activities. The system was previously validated [31] in a lab by comparing the response measured by the MEMS devices with conventional piezoelectric accelerometers. The most interesting results of the work are as follows:

1. As a MEMS sensor can measure gravity, the system could also be used as an inclinometer, a possibility that was verified with the corresponding test in the laboratory, with an ideal performance even in the presence of strong vibrations.
2. After all these developments and tests and their implementation on the construction site, in addition to providing the required service, which was to assist in real-time with codified alarm signals when the vibrations exceeded certain thresholds, it was possible to gain knowledge of this type of on-site activity, resulting in tangible values of the defined metrics: peak acceleration values, RMS values and tilt ratio. The thresholds proposed in Figure 3 complement some values reported by other researchers [12,13] working on the protection of cultural assets from mechanical loads. The nature and state of conservation of the different assets to be protected result in different thresholds that are hard to compare.
3. The hardware, specifically designed for the application, together with the on-demand software programming and the knowledge accumulated from continued use throughout the project, made it possible to know the acceleration levels of the different on-site works and thus adjust the alarm thresholds to practical levels. In this way, ensuring the integrity of the heritage asset to be safeguarded but also adequate progress of the works, the limit values of the different metrics, from which the different alarms were triggered, were adjusted. Figure 3 can be used as a reference for the thresholds involved in these dismantling activities, which have been set after handling the first panels.
4. Although the low-cost vibration-based warning system can be made more rugged and compact and even incorporate new sensors as anemometers, the experience has demonstrated that it was suitable for its intended use and has proved to be a very useful tool for the monitoring of the on-site work during its repeated use during months of operation.

In parallel to the described large-scale engineering project, this paper discusses how some on-site issues have been overcome, reporting on a case of study always of interest to the scientific community. Although the ad hoc vibration monitoring system is applied to the facade renovation workplace, its versatility facilitates its adaptation to other construction, restoration or deconstruction scenarios, helping to protect heritage assets without impacting occupational safety conditions.

Author Contributions: Conceptualization, A.L. and A.I.; methodology, J.J.V. and A.I.; software, J.J.V. and L.d.V.; validation, J.J.V., A.M. and A.I.; formal analysis, A.I. and A.M.; investigation, A.L. and A.I.; resources, A.I. and A.L.; data curation, A.M. and J.J.V.; writing—original draft preparation, A.L.; writing—review and editing, A.M. and L.d.V.; visualization, A.L. and L.d.V.; supervision, A.L. and A.I.; project administration, A.I.; funding acquisition, A.L. and A.I. All authors have read and agreed to the published version of the manuscript.

Funding: This research was funded by AEI, the Spanish government (10.13039/501100011033), and "ERDF A way of making Europe", grant number PID2022-140117NB-I00.

Data Availability Statement: The raw data supporting Section 5 (laboratory testing) of this article are available on request. All other data are subjected to authorisation by CAV Diseño e Ingeniería.

Acknowledgments: The authors would like to thank the company CAV Diseño e Ingeniería and the Fundación Santa María la Real del Patrimonio Histórico for their cooperative work.

Conflicts of Interest: The authors declare no conflicts of interest.

References

1. Park, J. Special Feature Vibration-Based Structural Health Monitoring. *Appl. Sci.* **2020**, *10*, 5139. [CrossRef]
2. Iban, N.; Soria, J.M.; Magdaleno, A.; Casado, C.; Diaz, I.M.; Lorenzana, A. Ad-Hoc Vibration Monitoring System for a Stress-Ribbon Footbridge: From Design to Operation. *Smart Struct. Syst.* **2018**, *22*, 13–25. [CrossRef]
3. Yarnold, M.; Salaman, S.; James, E. Deconstruction Monitoring of a Steel Truss Bridge. *Transp. Res. Rec. J. Transp. Res. Board* **2017**, *2642*, 139–146. [CrossRef]
4. Huang, X.; Xie, X.; Sun, J.; Zhong, D.; Yao, Y.; Tu, S. Monitoring and Analysis of the Collapse Process in Blasting Demolition of Tall Reinforced Concrete Chimneys. *Sensors* **2023**, *23*, 6240. [CrossRef]
5. Caetano, E.; Silva, S.; Bateira, J. A Vision System for Vibration Monitoring of Civil Engineering Structures. *Exp. Tech.* **2011**, *35*, 74–82. [CrossRef]
6. Karakostas, C.; Quaranta, G.; Chatzi, E.; Zülfikar, A.C.; Çetindemir, O.; De Roeck, G.; Döhler, M.; Limongelli, M.P.; Lombaert, G.; Apaydın, N.M.; et al. Seismic Assessment of Bridges through Structural Health Monitoring: A State-of-the-Art Review. *Bull. Earthq. Eng.* **2024**, *22*, 1309–1357. [CrossRef]
7. Pierleoni, P.; Marzorati, S.; Ladina, C.; Raggiunto, S.; Belli, A.; Palma, L.; Cattaneo, M.; Valenti, S. Performance Evaluation of a Low-Cost Sensing Unit for Seismic Applications: Field Testing During Seismic Events of 2016-2017 in Central Italy. *IEEE Sens. J.* **2018**, *18*, 6644–6659. [CrossRef]
8. Ribeiro, R.R.; Lameiras, R.D.M. Evaluation of Low-Cost MEMS Accelerometers for SHM: Frequency and Damping Identification of Civil Structures. *Lat. Am. J. Solids Struct.* **2019**, *16*, e203. [CrossRef]
9. Ragam, P.; Devidas Sahebraoji, N. Application of MEMS-based Accelerometer Wireless Sensor Systems for Monitoring of Blast-induced Ground Vibration and Structural Health: A Review. *IET Wirel. Sens. Syst.* **2019**, *9*, 103–109. [CrossRef]
10. Fu, M.; Liang, Y.; Feng, Q.; Wu, B.; Tang, G. Research on the Application of Multi-Source Data Analysis for Bridge Safety Monitoring in the Reconstruction and Demolition Process. *Buildings* **2022**, *12*, 1195. [CrossRef]
11. Keller, P.; McConnell, J.; Schumacher, T.; Thostenson, E.T. Construction Stress Monitoring Using a Wireless Sensor Network to Evaluate Reuse Potential of Structural Steel. *J. Struct. Eng.* **2019**, *145*, 04019143. [CrossRef]
12. Thickett, D. Vibration Damage Levels for Museum Objects. In Proceedings of the ICOM Committee for Conservation, 13th triennial Meeting, Rio de Janeiro, Brazil, 22–27 September 2002; ICOM: Rio de Janeiro, Brazil, 2002; pp. 90–95.
13. Kracht, K.; Kletschkowski, T. From Art to Engineering: A Technical Review on the Problem of Vibrating Canvas. Part I: Excitation and Efforts of Vibration Reduction. *Facta Univ. Ser. Mech. Eng.* **2017**, *15*, 163. [CrossRef]
14. Johnson, A.P.; Robert Hannen, W.; Zuccari, F. Vibration Control During Museum Construction Projects. *J. Am. Inst. Conserv.* **2013**, *52*, 30–47. [CrossRef]
15. *BS 5228-1*; Code of Practice for Noise and Vibration Control on Construction and Open Sites. Noise. BSI (British Standard Institution): London, UK, 2009.
16. *BS 7385-2*; Evaluation and Measurement for Vibration in Buildings. Guide to Damage Levels from Groundborne Vibration. BSI (British Stadard Institution): London, UK, 1995.
17. *DIN 4150-3*; Vibrations in Buildings—Part 3: Effects on Structures. DIN (Deutsches Institut für Normung): Berlin, Germany, 2016.

18. *BS 6472-1*; Guide to Evaluation of Human Exposure to Vibration in Buildings. Vibration Sources Other than Blasting. BSI (British Standard Institution): London, UK, 2008.
19. *ISO 2631-1*; Mechanical Vibration and Shock. Evaluation of Human Exposure to Whole-Body Vibration. Part 1: General Requirements. ISO (International Organization for Standardization): Geneva, Switzerland, 2008.
20. Wei, W.; Watts, S.; Seddon, T.; Crombie, D. Protecting Museum Collections from Vibrations Due to Construction: Vibration Statistics, Limits, Flexibility and Cooperation. *Stud. Conserv.* **2018**, *63*, 293–300. [CrossRef]
21. Johnson, A.; ElBatanouny, M. Vibrations and Museum Collections. Part 1: The Effects of Vibrations from Human Traffic and Construction on Museum Collections. *J. Preserv. Technol.* **2015**, *46*, 66–74.
22. Lucchi, E.; Buda, A. Urban Green Rating Systems: Insights for Balancing Sustainable Principles and Heritage Conservation for Neighbourhood and Cities Renovation Planning. *Renew. Sustain. Energy Rev.* **2022**, *161*, 112324. [CrossRef]
23. Wang, J. Exploring the Approaches of Adaptive Conservation, Reconstruction and Revitalization of Historic Districts A Case Study of Gunanjie Street in Dingshu, Yixing. *Archit. J.* **2021**, *5*, 1–7. [CrossRef]
24. Hou, W.; Liang, S.; Zhang, T.; Ma, T.; Han, Y. Low-Carbon Emission Demolition of an Existing Urban Bridge Based on SPMT Technology and Full Procedure Monitoring. *Buildings* **2023**, *13*, 1379. [CrossRef]
25. Seyed Khoei, A.; Akbari, R.; Maalek, S.; Gharighoran, A. Assessment of Design and Retrofitting Solutions on the Progressive Collapse of Hongqi Bridge. *Shock Vib.* **2020**, *2020*, 4932721. [CrossRef]
26. Murphy, B.; Locum, J.; Belser, M.; Bhegani, K.; Yarnold, M. Dead Load Evaluation through Truss Bridge Deconstruction Monitoring. *J. Bridge Eng.* **2018**, *23*, 04017115. [CrossRef]
27. Pirskawetz, S.; Steinbock, O.; Hille, F.; Schmidt, S.; Hofmann, D. Experiences from the Deconstruction of the Bridge Altstädter Bahnhof in the City of Brandenburg—Part 2: Damage Monitoring during Destructive Tests. *Beton-Und Stahlbetonbau* **2022**, *117*, 581–589. [CrossRef]
28. Hu, X.; Zhou, Y.; Vanhullebusch, S.; Mestdagh, R.; Cui, Z.; Li, J. Smart Building Demolition and Waste Management Frame with Image-to-BIM. *J. Build. Eng.* **2022**, *49*, 104058. [CrossRef]
29. Obi, L.; Awuzie, B.; Obi, C.; Omotayo, T.; Oke, A.; Osobajo, O. BIM for Deconstruction: An Interpretive Structural Model of Factors Influencing Implementation. *Buildings* **2021**, *11*, 227. [CrossRef]
30. Terenzi, G.; Fuso, E.; Sorace, S.; Costoli, I. Enhanced Seismic Retrofit of a Reinforced Concrete Building of Architectural Interest. *Buildings* **2020**, *10*, 211. [CrossRef]
31. Magdaleno, A.; Villacorta, J.J.; del-Val, L.; Izquierdo, A.; Lorenzana, A. Measurement of Acceleration Response Functions with Scalable Low-Cost Devices. An Application to the Experimental Modal Analysis. *Sensors* **2021**, *21*, 6637. [CrossRef] [PubMed]
32. Żak, P. Using 9-Axis Sensor for Precise Cardiosurgical Robot Master Angular Position Determination. *Solid State Phenom.* **2013**, *199*, 356–361. [CrossRef]
33. Kanters, J. Design for Deconstruction in the Design Process: State of the Art. *Buildings* **2018**, *8*, 150. [CrossRef]
34. *IEC 60529*; Degrees of Protection Provided by Enclosures (IP Code). NEMA (National Electrical Manufacturers Association): Rosslyn, VA, USA, 2004.
35. Savage, P.G. Strapdown Inertial Navigation Integration Algorithm Design Part 1: Attitude Algorithms. *J. Guid. Control Dyn.* **1998**, *21*, 19–28. [CrossRef]
36. Ha, D.; Park, H.; Choi, S.; Kim, Y. A Wireless MEMS-Based Inclinometer Sensor Node for Structural Health Monitoring. *Sensors* **2013**, *13*, 16090–16104. [CrossRef]